

Manuscript Number:

Title: INTERPRETATION OF THE EXPERIMENTALLY MEASURED DYNAMIC RESPONSE OF AN
EMBEDDED RETAINING WALL BY FINITE ELEMENT MODELS

Article Type: MetroGeotechnics Papers

Keywords: Diaphragm wall, Model refinement, Dynamic properties, System identification.

Corresponding Author: Dr. Filippo Santucci de Magistris, PhD

Corresponding Author's Institution: University of Molise

First Author: Carlo Rainieri

Order of Authors: Carlo Rainieri; Arindam Day; Giovanni Fabbrocino, Professor; Filippo Santucci de Magistris, PhD

Abstract: Experimental measurements of the ambient vibration response of an embedded retaining wall were used to enhance the understanding of the dynamic behavior of this typology of geotechnical systems. The experimental estimates of the dynamic properties of the soil-wall system made possible the refinement of a numerical model, originally set according to standard geotechnical investigations, by means of sensitivity analyses with respect to a few model parameters. As a result, a representative model of the dynamic behavior of the soil-wall system in operational conditions was obtained. It yielded a significant insight into the soil-structure interaction mechanisms. Under low acceleration field, a superposition principle was validated, resulting in a potential a priori estimation of the response of the overall system based on the knowledge of the decoupled responses of different domains bounded by the excavation and the wall.

Suggested Reviewers: Luigi Di Sarno
Dipartimento di Ingegneria, University of Sannio
ldisarno@unisannio.it
well-known researcher in Earthquake Engineering

Augusto Penna
Dipartimento di Ingegneria, University of Sannio
apenna@unisannio.it
well-known expert of Earthquake Geotechnical Engineering

Giacomo Russo
Dipartimento di Ingegneria Civile e Meccanica, University of Cassino and Southern Lazio
giarusso@unicas.it
Well known expert in Geotechnical Engineering



Filippo Santucci de Magistris, *Ph.D.*
filippo.santucci@unimol.it Tel: +39 0874404935

Campobasso, 22.06.2015

Dear Prof. Grattan,
Dear Guest Editors,

please consider the paper “Interpretation of the experimentally measured dynamic response of an embedded retaining wall by finite element models” by Carlo Rainieri et al. for possible publication in the special issue MetroGeotechnics of the journal Measurement.

Regards

Dr. Filippo Santucci de Magistris
(Associate Professor of Geotechnical Engineering)



**INTERPRETATION OF THE EXPERIMENTALLY MEASURED DYNAMIC
RESPONSE OF AN EMBEDDED RETAINING WALL BY FINITE
ELEMENT MODELS**

Carlo Rainieri^{*1}, Arindam Dey[#], Giovanni Fabbrocino^{*2}, Filippo Santucci de Magistris^{*3}

^{*1}Post doctoral Fellow, ^{*2}Full Professor, ^{*3}Associate Professor
Structural and Geotechnical Dynamics Laboratory *StreGa*
Department of Biosciences and Territory, University of Molise
Via De Sanctis s.n.c. – 86100 Campobasso (CB), Italy
Tel. +39 0874 404883, Fax 0874-404952,
Corresponding author's e-mail: giovanni.fabbrocino@unimol.it

[#]Assistant Professor
Indian Institute of Technology Guwahati
Department of Civil Engineering, Guwahati 781039,
Assam, India
E-mail: arindam.dey@iitg.ernet.in

ABSTRACT

Experimental measurements of the ambient vibration response of an embedded retaining wall were used to enhance the understanding of the dynamic behavior of this typology of geotechnical systems. The experimental estimates of the dynamic properties of the soil-wall system made possible the refinement of a numerical model, originally set according to standard geotechnical investigations, by means of sensitivity analyses with respect to a few model parameters. As a result, a representative model of the dynamic behavior of the soil-wall system in operational conditions was obtained. It yielded a significant insight into the soil-structure interaction mechanisms. Under low acceleration field, a superposition principle was validated, resulting in a potential a priori estimation of the response of the overall system based on the knowledge of the decoupled responses of different domains bounded by the excavation and the wall.

Keywords: Diaphragm wall, Model refinement, Dynamic properties, System identification.

1 INTRODUCTION

Rigid or flexible retaining walls, such as gravity, cantilever or embedded walls usually support deep excavations, bridge abutments or harbor-quays. The behavior of gravity retaining walls under static conditions is investigated in detail over the years, starting from the rational development of earth pressure theories, which date back to the classical works of Coulomb [1] and Rankine [2]. Their seismic design is also already established and is traditionally based on an extension of Coulomb's limit equilibrium analysis, commonly known as the Mononobe-Okabe method [3, 4].

The Mononobe-Okabe theory was widely discussed (see, for instance, [5, 6, 7, 8] and the key references listed in [9]) and it is, nowadays, the most common design method among practitioners. It is especially used in the form presented by Seed and Whitman [10], which can be found in many codes and regulations [11, 12, 13]. Notwithstanding the widely accepted use of this method, Ebeling and Morrison [14] asserted: "*A small number of model testing programs have filled in some of the blanks in the understanding of dynamic response of retaining -structures. Theoretical studies have been made, but with very limited opportunities to check the results of these calculations against actual, observed behavior. As a result, there are still major gaps in knowledge concerning proper methods for analysis and design*". These words appear to be still valid and particularly appropriate for embedded retaining walls. Under dynamic excitations, the different components of the retaining system exhibit complex and interdependent responses, which can be roughly summarized as follows:

- (a) dynamic interaction between the wall, the retained backfill and the soil in front of the wall;
- (b) dynamic interaction of the underlying soil with the sustained structure.

These aspects and the effects of damping, natural frequencies of the system, phase lags and amplifications within the backfill on the system response cannot be properly analyzed by means of simplified approaches, such as the Mononobe-Okabe method.

Advanced dynamic analysis represents a more refined, but even more complex examination tool. Dynamic analyses by means of finite-difference or finite-element methods can take into

1 detailed account of the soil-structure interaction, so they are, potentially, the most effective
2 techniques to predict the response of a flexible retaining wall. However, in the absence of
3 systematic studies and criteria for validation of the results provided by such dynamic analyses (for
4 instance, through their correlation to accurate and reliable experimental data), the effectiveness of
5 the tool remains largely dependent on the engineering judgment.

6 Giarlelis and Mylonakis [15] propose a study about the dynamic properties of a cantilever wall.
7 In particular, a Dynamic linear Wall-Soil-Structure Interaction (DWSSI) analysis was carried out to
8 investigate the effect of the presence of the cantilever wall and its flexibility on the induced
9 acceleration of the retained soil. Transfer functions were derived from the acceleration profiles of
10 the wall, allow estimating the natural frequencies of vibration of the system. In any case, simplified
11 geotechnical models in terms of geometry and material properties were considered. Moreover, they
12 do not take advantage of any verification or calibration based on the results of experimental, full
13 scale, in situ dynamic measurements. This limitation can be probably associated to the fairly limited
14 availability of experimental investigations about the dynamics of walls in the literature. Amano et al.
15 [16] execute free and forced full-scale vibration tests on a quay wall in Japan. Fukuoka and
16 Imamura [17] measure earth pressures and accelerations in the case of cantilever, large concrete
17 block and multiple anchored retaining walls during real Japanese earthquakes. Elgamal et al. [18]
18 install a shaker in the backfill of a cantilever retaining wall and analyze the forced vibrations of the
19 system. In any case, all these researches refer to gravity or cantilever walls, while no full-scale data
20 seem to be available about embedded retaining walls. In spite of the research efforts devoted to the
21 analysis of the dynamic response of retaining walls, the above-mentioned references reveal that
22 there is a substantial lack of knowledge about the dynamic properties and response of embedded
23 retaining systems, even in the presence of low amplitude excitations. On the other hand, it is worth
24 noting that results of dynamic analyses heavily depend on the reliability of the model in terms of
25 geometry and input parameters (boundary conditions, material properties, and so on). Thus,
26 extensive geotechnical investigations and the availability of full scale dynamic measurements are

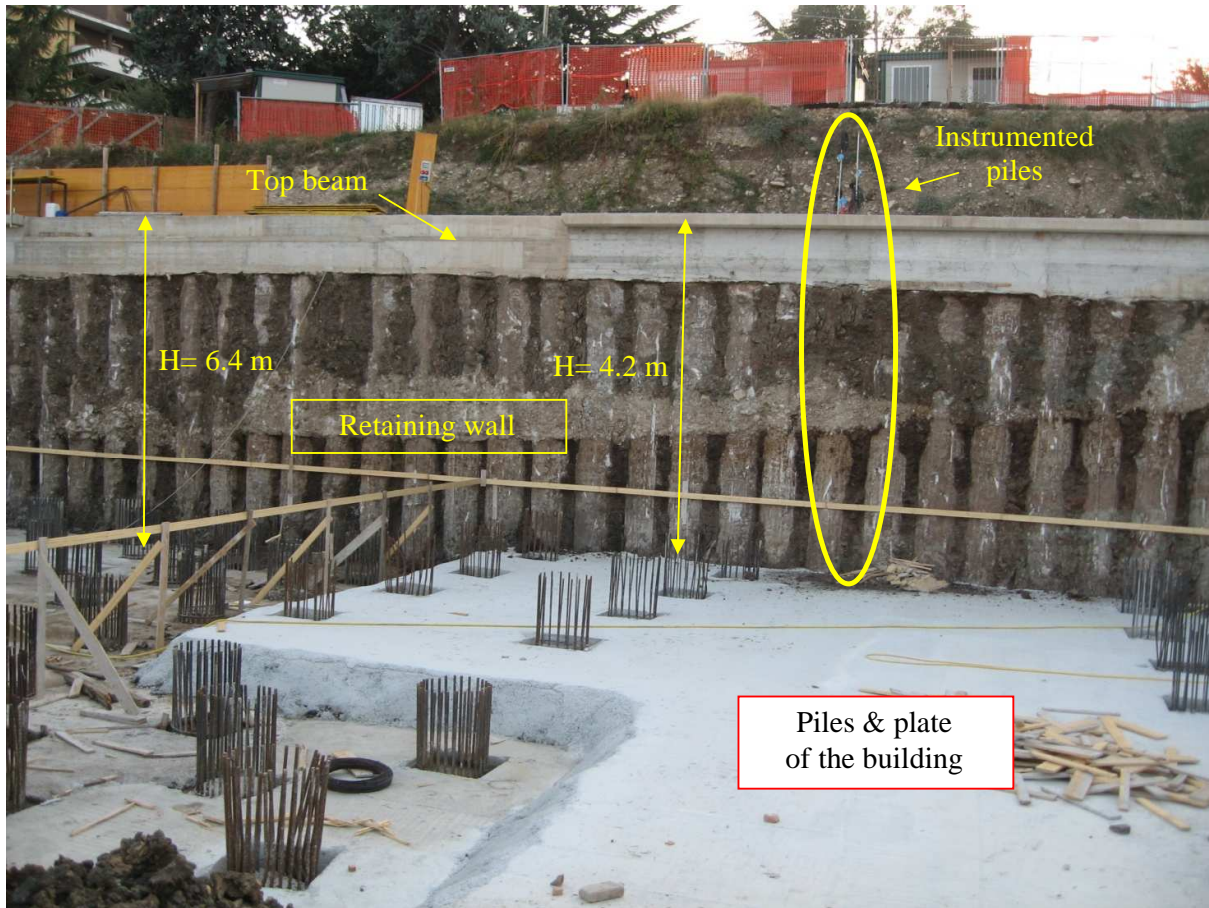
certainly useful for the setting and calibration of effective numerical models of the soil-wall system under operational conditions in view of more sophisticated analyses.

The opportunities provided by dynamic measurements on a real embedded retaining wall for the refinement of its numerical model are the main topic of the present paper, which takes into account the above-mentioned technical background and open issues. Herein it is shown, in particular, how the model refinement, founded on the available measurement of the soil-wall natural frequencies, can provide an insight on the most relevant geotechnical parameters affecting the dynamic response of the system under investigation in operational conditions. The paper is organized as follows. Setting of a basic Finite Element (FE) model of the soil-wall system based on data is presented first, and various pertinent issues referring to the main uncertainties in its development are discussed (Section 2 and Section 3). Then, the refinement of the numerical model based on the results of ambient vibration tests is described in detail (Section 4), drawing some interesting conclusions about the soil-structure interaction mechanisms at low amplitude vibrations.

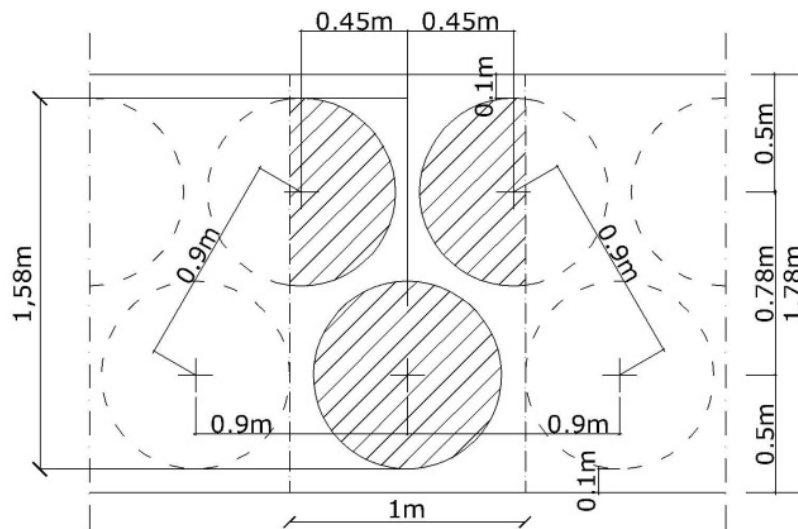
2 EXPERIMENTAL CHARACTERIZATION OF THE GEOTECHNICAL SYSTEM

The analyzed reinforced concrete (r.c.) embedded retaining wall (**Figure 1a**) is a part of the new Students' Residence at the University of Molise in Campobasso, Italy. It consists of two alignments of adjacent but not contiguous piles (**Figure 1b**). These have a diameter of 800 mm and a length of 18 m. The free height of the wall is 6.4 m. An r.c. beam, whose cross section is 1.0 m high, connects the heads of the piles; there are no anchorages. The herein reported measurements and analyses refer to a time before the construction of the nearby building.

Deposits of varicolored scaly stiff clays, with alternate beds of limestone, calcareous marls and sandy materials, and supplementary presence of calcarenite and fragments of San Bartolomeo's flysch, characterized the site from a geological point of view. The upper layer is constituted by remolded debris cover of anthropogenic origin, whose thickness varies between 4 and 10 m. **Figure 2a** shows the geological map of the area.



(a)



(b)

- 1 **Figure 1.** Picture view of part of the geotechnical works for the New Students' Residence in
- 2 Campobasso (a); layout of the equivalent sheet pile cross section, plan view (b)

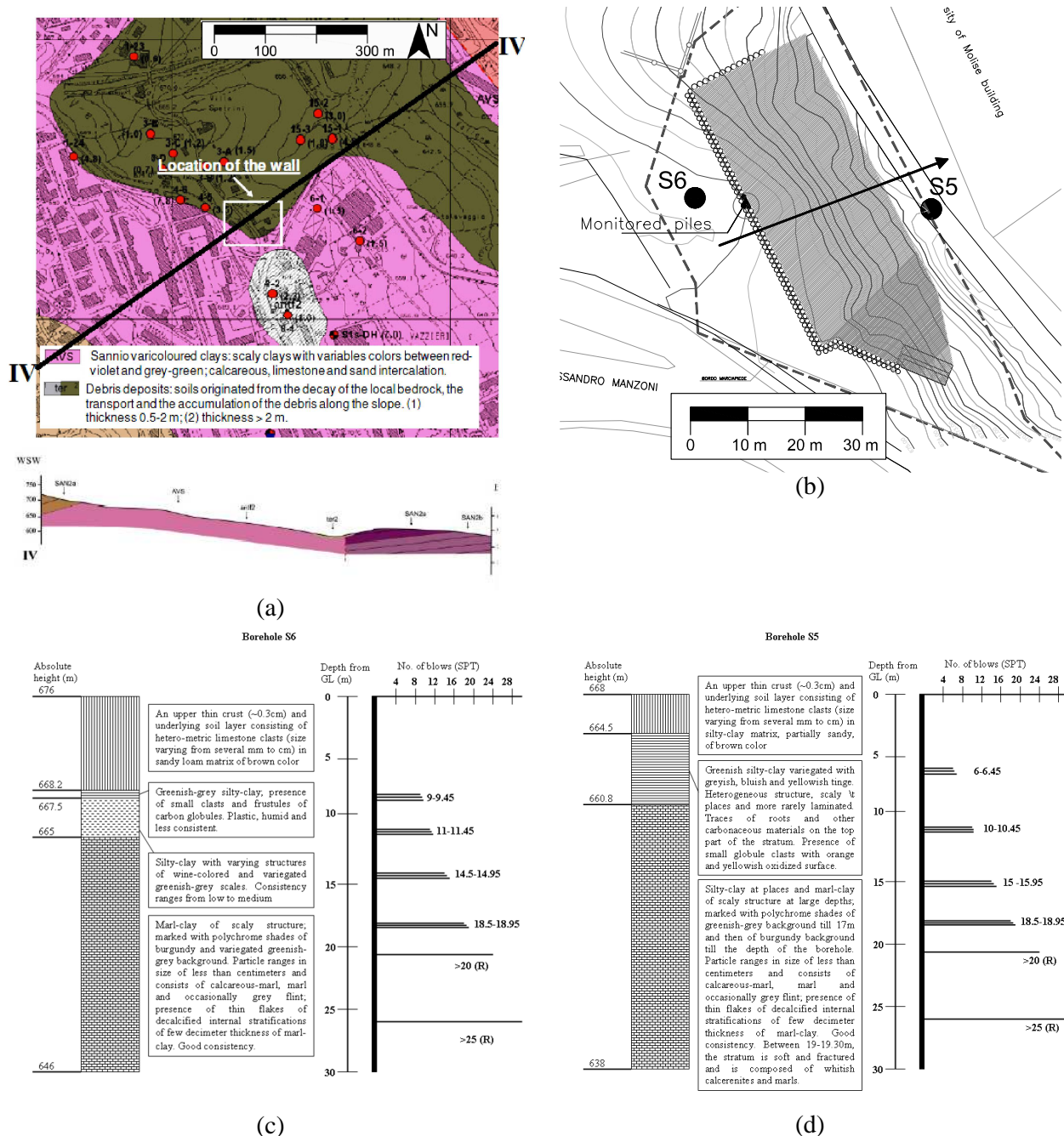


Figure 2. Geological map and section of the Vazzieri area in Campobasso. AVS – Varicoloured scaly clays; *ter2* – Deposits of debris cover; *anf2* – Anthropogenic remolded covering; *SAN2* – San Bartolomeo's Flysch deposit (a); schematic location of boreholes and retaining wall on a contour plot; the general direction of slope in the locality is indicated by the arrow (b); characteristics of strata and SPT test results for Borehole S6 (c) and Borehole S5 (d)

The team of Professional Engineers who designed the Residence according to relevant Italian codes also carried out the geotechnical characterization of the site. It was based on two borehole investigations (S5 and S6) performed on both sides of the retaining wall. **Figure 2b** schematically

shows the positions of the boreholes and the retaining wall. The arrow indicates the general direction of the slope in the investigated area. The borehole investigations were carried out up to a depth of 30 m from the ground level. Stratigraphic Column Extractions, Standard Penetration Tests (SPT) and Down-Hole tests (DH) were executed. Laboratory tests to determine the main physical and mechanical properties of the soil were performed on the extracted samples. The strength parameters of the soil samples were determined by triaxial and direct shear tests. **Figure 2c** and **Figure 2d** show the different soil layers, as identified according to the stratigraphical characteristics and the SPT blow counts. Down-hole tests carried out in the two boreholes provided the primary and shear wave velocities (V_p , V_s) profiles. Estimates of the Poisson's ratio, modulus of elasticity and shear modulus under dynamic conditions were then obtained according to the following well-established expressions (see, for instance, Richart et al. [19]):

$$\nu = \frac{0.5 \cdot (V_p/V_s)^2 - 1}{(V_p/V_s)^2 + 1}; \quad E = \frac{\gamma}{g} \cdot V_p^2 \cdot \frac{(1+\nu) \cdot (1-2\nu)}{(1-\nu)}; \quad G = \frac{E}{2 \cdot (1+\nu)} \quad (1)$$

The variation of the shear wave velocity with depth is reported in **Figure 3**.

As indicated in **Figure 2b**, since the boreholes are located along the general direction of the slope in the area, there exists a grade difference of about 8 m at the ground level between them. The excavation of the borehole S6 started from an absolute height of about 676 m, while that of borehole S5 commenced from nearly 668 m (**Figure 3**). The boreholes were separated by a longitudinal distance of about 35 m. Examination of the data has led to recognize the presence of soil layers with nearly identical characteristics but at a certain difference in elevation. An inclined stratigraphy with an approximate slope (1V:10H) was therefore adopted for the geometry of the geotechnical model. This was incorporated in the numerical model of the soil-wall system, which is described in the next section.

In order to obtain reference values of the dynamic properties of the wall in view of the refinement of the numerical model, an ambient vibration test was carried out. To this aim it is worth mentioning that two piles of the wall are equipped with six couples of embedded accelerometers,

installed according to two orthogonal directions (parallel to the pile axis and orthogonal to the wall surface) at different positions along the height. Such sensors are part of a permanent seismic monitoring system [20, 21].

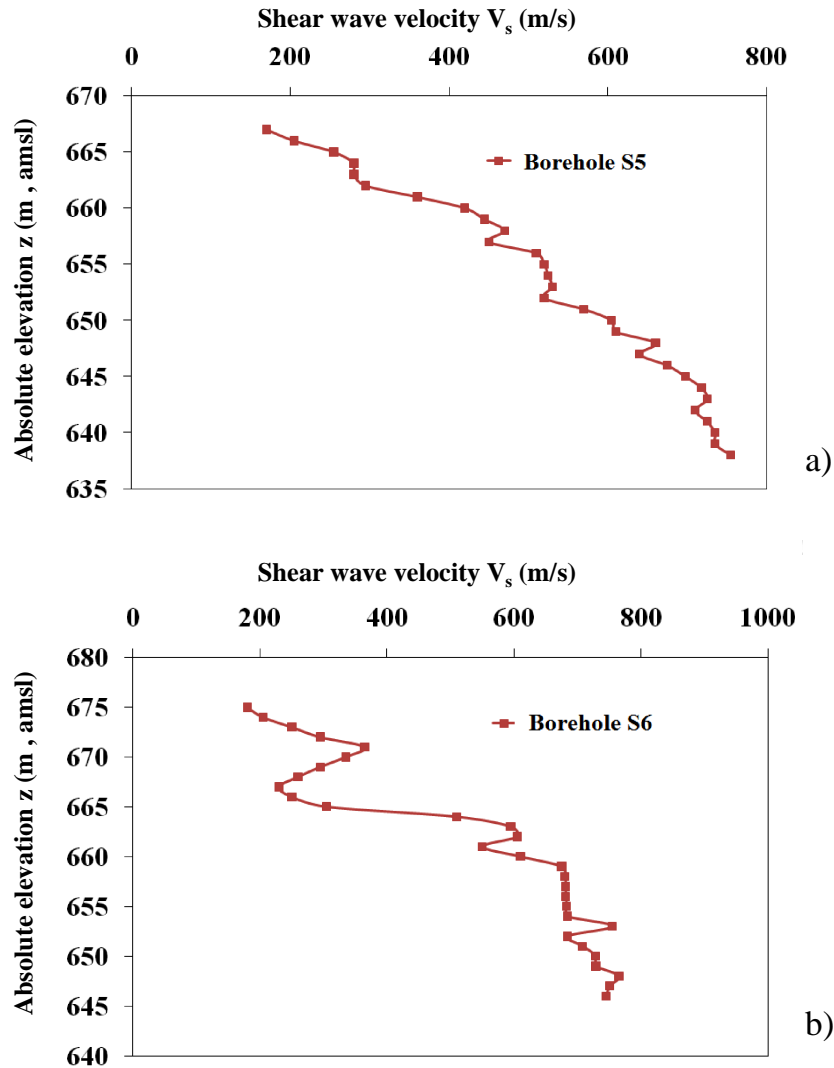


Figure 3. Shear wave velocity profile obtained from borehole S5 (a) and borehole S6 (b)

Even if the embedded sensors are able to measure also the ambient vibrations, because they are low-noise, high sensitivity (10 V/g) accelerometers, they are not enough in number to observe the deflection shape of the wall with adequate spatial resolution. Thus, additional five accelerometers with the same characteristics were externally mounted along the free height of the wall. This provided an improvement of the spatial resolution of measurements in the upper part of the wall, which is also characterized by the largest displacements. The additional sensors were equally

spaced at a distance of 0.8 m. **Figure 4** shows a picture of the final sensor layout, including the externally mounted as well as the embedded sensors. The horizontal accelerations were therefore measured in eight positions along the height. The ambient vibration response of the wall was acquired for one hour at a sampling rate of 100 Hz.

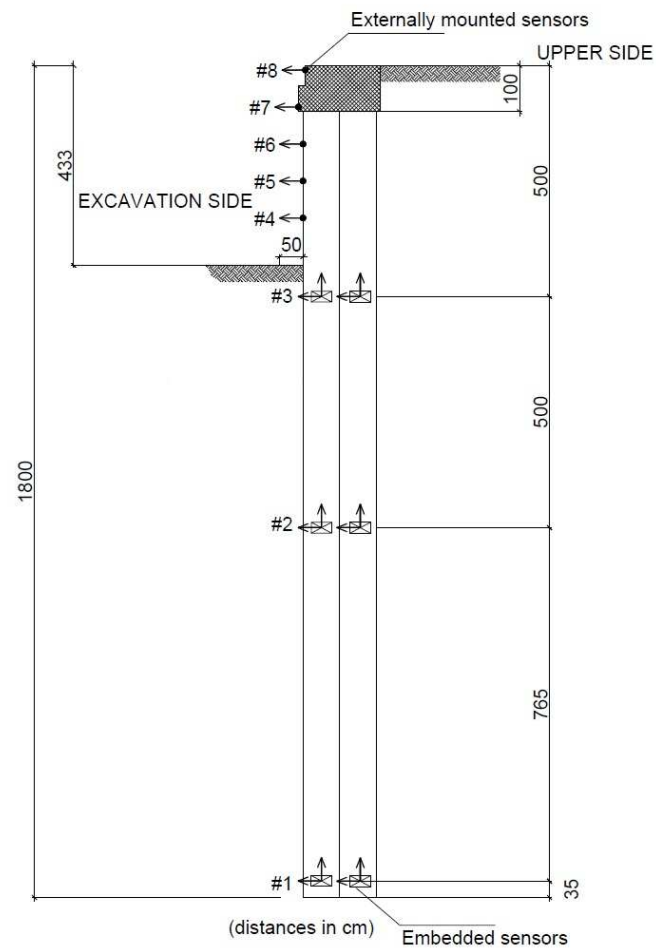


Figure 4. Sensor layout

The ambient vibration response of the wall was analyzed by powerful and robust Operational Modal Analysis (OMA) techniques, such as the Frequency Domain Decomposition (FDD) [22, 23] and the Stochastic Subspace Identification (SSI) [23, 24, 25].

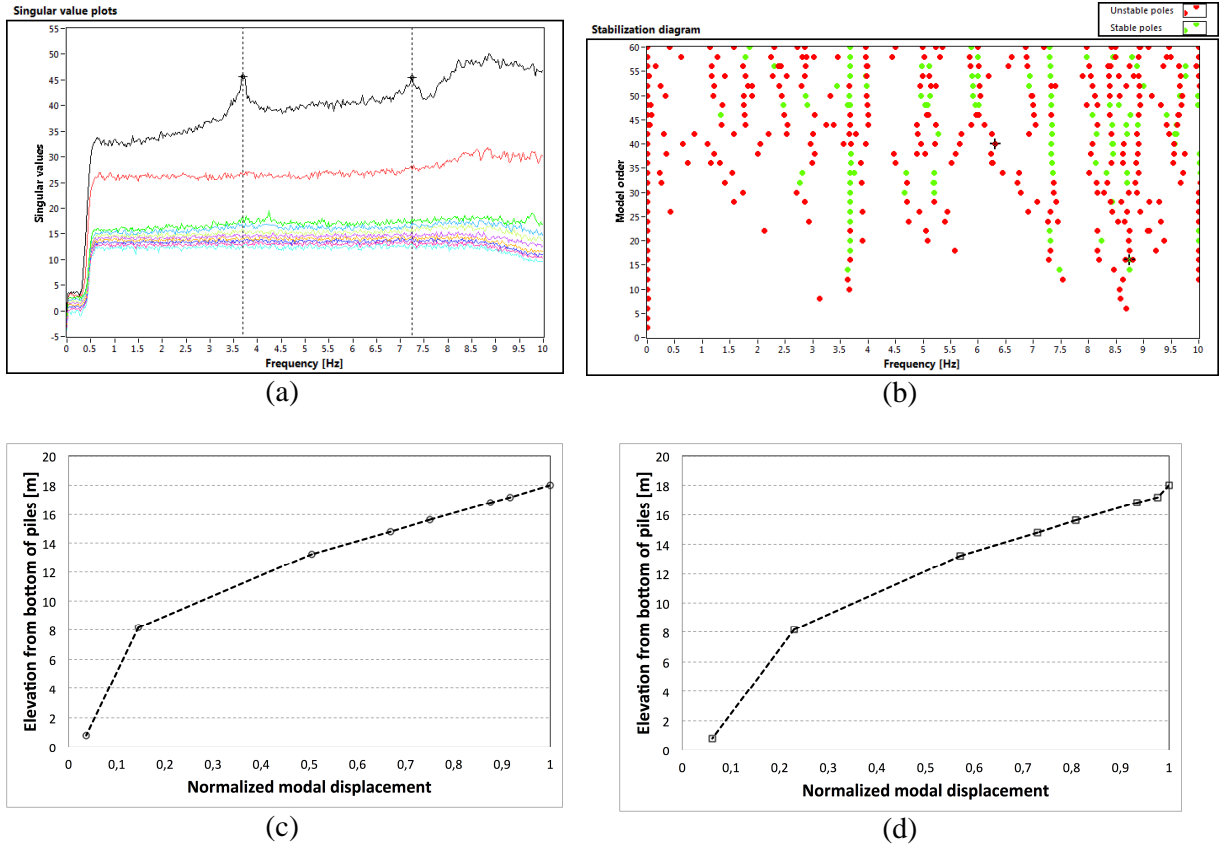


Figure 5. Analysis of the ambient vibration response of the wall: Singular value plots from the FDD method (a), stabilization diagram from the SSI method (b), first experimental mode shape (c), second experimental mode shape (d)

The FDD is a frequency domain, non-parametric, output-only modal identification technique based on the Singular Value Decomposition (SVD) of the output Power Spectral Density (PSD) matrix. Structural resonances are identified from the singular value plots through peak picking; the corresponding singular vector is a good estimate of the mode shape. The SSI, conversely, is a time domain, parametric, modal identification procedure based on a state-space description of the dynamic problem. The modal parameters are extracted from realizations of the state matrix and output matrix of the system obtained from measurements of its response to ambient vibrations through projections and other algebraic operators.

Before processing, data pre-treatment was conducted to validate the quality of the data and the absence of errors or anomalies, such as clipping, drop-out, noise spikes and so on. Hanning window and 66% overlap were used for the spectrum computation. A frequency resolution of 0.01

Hz was obtained. The results are summarized in **Table 1**, while the Singular Value Plots provided by the FDD procedure and the stabilization diagram resulting from SSI are shown in **Figure 5a** and **Figure 5b**. The estimated mode shapes are shown in **Figure 5c** and **Figure 5d**.

Mode	f_{exp} (Hz)	ξ_{exp} (%)
I	3.68	1.4
II	7.23	1.2

Table 1. Experimental estimates of natural frequencies and damping ratios in operational conditions

The reliability of the obtained results was confirmed by cross-checks in terms of both natural frequencies and mode shape estimates. Consistent results, characterized by negligible scatter, were obtained from the two OMA methods, thus ensuring the success of the identification process. Such results can be profitably used to refine the numerical model that was set to investigate the dynamic behavior of the soil-wall system, as discussed in the next section.

3 BASIC NUMERICAL MODEL FOR MEASUREMENT INTERPRETATION

A Finite Element (FE) model of the soil-wall system was set using Plaxis 2D v. 8.4 Dynamics Module [26] in order to evaluate its behavior under operational conditions.

The geometry of the basic FE model of the soil-wall system is depicted in **Figure 6a**. To assess the correlation between the dynamic properties of the system as provided by the FE model and the results of dynamic identification tests under operational conditions, the soil was modeled as linear elastic (LE), in compliance with the assumption of low amplitude of the ambient vibrations. The elastic parameters for each stratum were estimated from the results of the geotechnical investigations described in the previous section. The embedded retaining wall was modeled by a plate element of finite thickness. The stiffness of the piles-beam system was evaluated by considering a 1 m large strip of the wall, including two piles (**Figure 1b**). Since, the sheet pile wall is comprised of two alignments of non-contiguous piles, the axial and bending stiffness of the overall system lies in between the stiffness of a single pile and the aggregated value of two

contiguous piles connected by the top beam. The adopted scaled down values are: axial stiffness (EA) = 3.08×10^7 kN/m, and bending stiffness (EI) = 4.76×10^6 kNm²/m. The equivalent thickness of the plate element (d_{eq}) is evaluated by the following expression: $d_{eq} = \sqrt{12 * EI / EA}$, and a value of 1.362 m was adopted for the same in the model. A no-slip debonding condition was assumed at the soil-wall interface. The water table was below the model, as resulting from the geotechnical investigations. **Table 2** summarizes the adopted soil and wall parameters for the basic model.

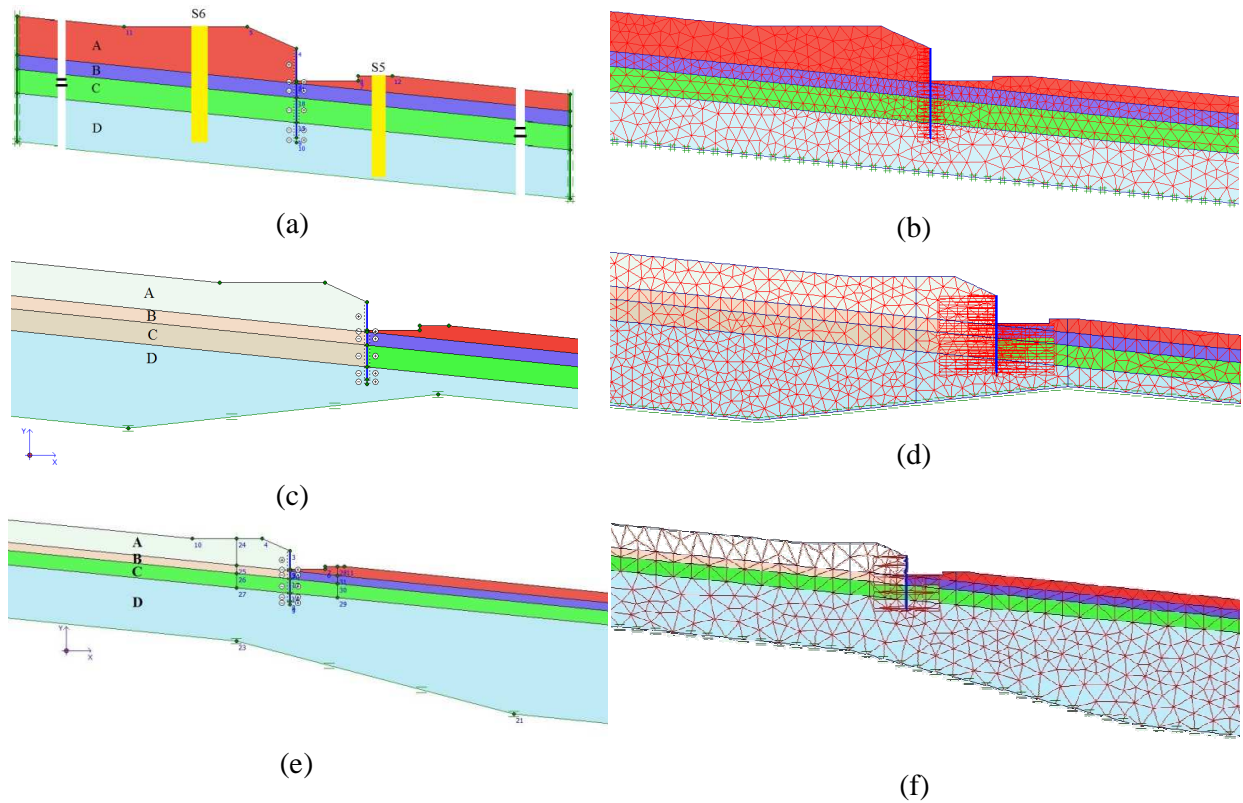


Figure 6. Views of the FE models in the region around the wall: Geometry of the basic FE model (a) and its zoomed meshing (b); zoomed view of the FE model geometry after the first refinement (c) and its meshing (d); zoomed view of the FE model geometry after the second refinement (e) and its meshing (f)

Soil Layer	Material Type	E_0 (10^5 kPa)	G_0 (10^5 kPa)	ν	γ (kN/m ³)	V_s (m/s)	H_L (m) Left of wall	H_R (m) Right of Wall
A	LE	3.188	1.113	0.432	18.00	246.2	8	3
B	LE	4.086	1.433	0.426	19.03	271.6	3	3
C	LE	14.51	5.045	0.438	19.47	503.9	5	5
D	LE	26.49	9.243	0.433	19.98	673.3	10	10

Table 2 Material properties of soil adopted in the basic FE model

1 Before the evaluation of the correlation between numerical and experimental results, the model
2 was optimized in order to obtain its best functionality. A basic guidance to the selection of
3 appropriate numerical parameters, so that the reliability and accuracy of the predictions are not
4 jeopardized, is reported in the following. Further suggestions about analysis parameter settings are
5 given in [26].

6 A fairly accurate model was set in compliance with appropriate guidelines reported in the
7 literature and proved by the results of a series of dynamic analyses of vertical propagation of S-
8 waves in an homogeneous layer using Plaxis 2D v. 8.4 Dynamic module [27]. Those approaches
9 allow to properly account for the influence of boundary conditions, meshing and damping
10 parameters on the response of the system A domain aspect ratio of 40 (ratio of total domain width to
11 the average height) was chosen, after a trial and error procedure to fulfill the assumption of semi-
12 infinite soil.

13 Absorbent boundaries were used setting the relaxation coefficients as follows: $C_1=1$ and
14 $C_2=0.25$ [28].

15 The criteria reported in [29] were adopted to determine the mesh size, and a suitable refined
16 meshing scheme was accordingly set. **Figure 6b** portrays the adopted meshing for the mentioned
17 numerical model.

18 In order to extract the dynamic properties of the model of the soil-wall system, a Gaussian
19 white noise (duration: 1 hour; sampling frequency: 100 Hz) and an impulse load were alternatively
20 applied as input, so that all the modes in the frequency range of interest were almost equally excited
21 [30]. The excitation was applied as propagating shear waves generated by base shaking and a
22 dynamic analysis of the basic model was carried out to determine the acceleration responses of the
23 retaining wall at different locations, corresponding to the positions of the sensors in the
24 experimental tests. Numerical damping parameters [31, 32] affect the amplification of the response
25 at resonances but not the shape of the amplification function. An implicit Newmark scheme governs
26 the numerical time-integration and Newmark damping parameters specifies numerical damping. An

Undamped Newmark Scheme, also known as average acceleration scheme, was considered (so that the predicted frequency spectra suffer minimal effect from numerical damping) with the following parameters: $N_\alpha=0.25$ and $N_\beta=0.5$. Rayleigh damping is used to simulate material damping under plane-strain conditions. Rayleigh parameters were determined following the Park and Hashash approach [33]. Considering a 1% damping on the overall system in agreement with the experimental estimates (**Table 1**), Rayleigh damping parameters were set as follows: $R_\alpha=0.293$ and $R_\beta=3.032\text{E-}4$, both for the soil and the wall. The fundamental dynamic properties of the model were then extracted by conventional input-output dynamic identification techniques [34], such as the deterministic subspace identification [23]. The dynamic properties of the modeled system were finally compared with the corresponding experimental estimates obtained from field dynamic measurements. The values of the fundamental resonant frequencies of the basic numerical model of the wall were equal to 4.7 Hz and 6.7 Hz, respectively. Since these values were slightly different from the corresponding experimental estimates, as reported in **Table 3**, a refinement of the FE model to more closely match the experimental results was needed. The process for minimization of the scatter between experimental observations and numerical predictions is described in detail in the next section.

Basic model			
Mode	f_{exp} (Hz)	f_{FEM} (Hz)	Scatter (%)
I	3.68	4.7	21.7
II	7.23	6.7	-7.33
First refinement			
Mode	f_{exp} (Hz)	f_{FEM} (Hz)	Scatter (%)
I	3.68	3.64	-1.1
II	7.23	7.46	3.1

Table 3. Comparisons between experimental and numerical estimates of the natural frequencies: the basic FE model and the FE model after the first refinement

4 MODEL REFINEMENT

4.1 SELECTION OF THE UPDATING PARAMETERS

Modification of the model parameters and assumptions can be carried out to minimize discrepancies between numerical predictions and experimental results. A classical approach in this direction would be a trial-and-error scheme; however, when it is mostly governed by the random changes in the contributory factors, it is highly tedious, time-consuming and often based on intuitions rather than justified by a mathematical and logical approach. As alternatives, some robust computational procedures were developed over time, to achieve the same in a regularized manner. In particular, experimental estimates of dynamic properties (natural frequencies and mode shapes) are being largely used for model parameter adjustments, especially in the field of structural engineering. A detailed discussion about model updating procedures and some applications can be found elsewhere [35, 36].

In this section, the main uncertainties affecting the numerical model of the soil-wall system are identified and the process for the minimization, in a regularized manner, of the scatter with the reference experimental results is described. In particular, the model refinement aimed at optimizing the correlation with the experimental results, quantified by the frequency scatter:

$$\Delta f = \frac{f_{i,FEM} - f_{i,exp}}{f_{i,exp}} \cdot 100 \quad i=1, 2 \quad (2)$$

(where $f_{i,FEM}$ and $f_{i,exp}$ are the numerical and experimental value of the natural frequency of the i -th mode, respectively) and the mode shape correlation expressed by the MAC index [37]:

$$MAC(\{\phi_{i,FEM}\}, \{\phi_{i,exp}\}) = \frac{|\{\phi_{i,FEM}\}^T \{\phi_{i,exp}\}|^2}{(\{\phi_{i,FEM}\}^T \{\phi_{i,FEM}\})(\{\phi_{i,exp}\}^T \{\phi_{i,exp}\})} \quad i=1, 2. \quad (3)$$

$\{\phi_{i,FEM}\}$ and $\{\phi_{i,exp}\}$ are the numerical and experimental mode shape vectors for the i -th mode, respectively; the superscript T denotes transpose.

Regarding the uncertainties in the model geometry, it is worth noting that the above-mentioned boreholes, S5 and S6, each 30 m deep, though allow for a reasonable identification of the soil stratigraphy for design purposes, do not provide enough insight about the depth and profile of the bedrock. However, its location has significant influence on the dynamic response of the model. Since most of the model parameters are directly measured from in-situ and laboratory tests on soil, the indirect identification of the bedrock depth and profile was selected as a target of the refinement process. Sensitivity analyses showed that the results are fairly dependent to these parameters, which are, at the same time, the most uncertain, as pointed out also by the results of SPT tests. In fact, SPT blow-counts of boreholes S5 and S6 reveal a refusal of penetration at 20 m and 26 m, but, the borehole is excavated further until 30 m. Hence, it is very difficult to adjudge the soil at this depth to be or not as a part of the bedrock. Moreover, results from the two borehole investigations are actually not sufficient to describe the global profile of the substrata along the direction orthogonal to the wall; as a consequence the boreholes provide only a glimpse of the local stratigraphy. On the contrary, the dynamic response of the soil-wall system is definitely affected by the substrata profile. For further clarification about soil geometry, borehole investigations in the nearby vicinity of the study-area were also inspected. They seem to show the presence of hard soils on the excavated side at a depth of about 15 m, as depicted in [Figure 7](#), but there is no evidence of the presence of the bedrock. Even less information is available about the soil behind the wall, due to a lack of investigative explorations. The already mentioned borehole S6 provides the only instance. Since there is a lack of information and a significant grade difference between the stratigraphic profile of the soils in the back and in front of the wall, it is quite difficult to verify the depth of the bedrock, in particular on the backfill side, or adjudge the irregularity in the profile of the bedrock across the transverse direction of the wall according only to the results of in-situ investigations.

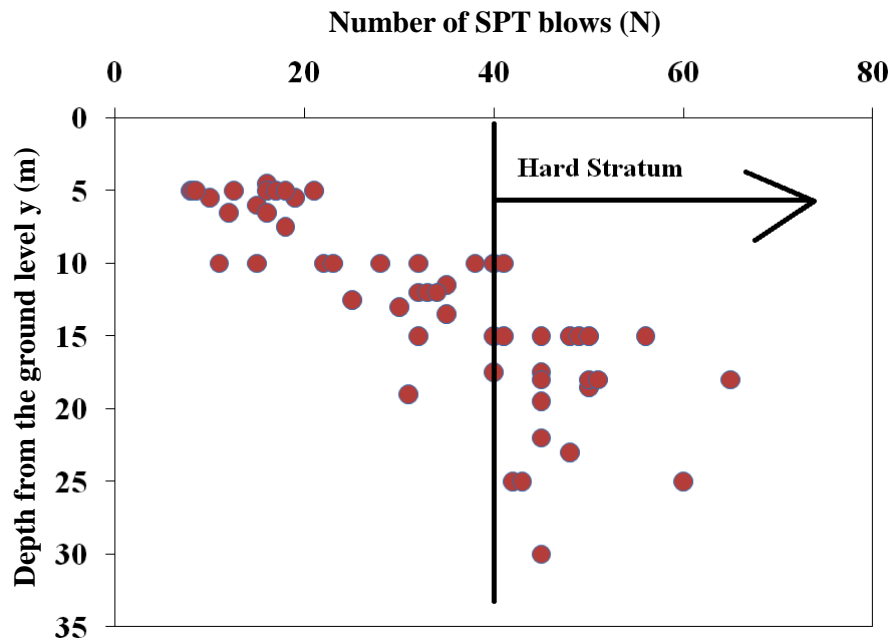


Figure 7. Conglomerated plot of SPT blow-counts from the nearby boreholes towards the soil in front of the wall as a function of depth from the ground level

As a consequence, the refinement process had the identification of the depth and the profile of the bedrock as a primary concern. After that, minor refinements were obtained by properly setting the elastic parameters of the two upper layers on the backfill side of the wall. In fact, inspection of [Figure 3](#) points out also that the shear wave profile from borehole S6 is more scattered than the same from S5, especially within 16 m from the ground level. Taking into account that the rotation of the wall due to excavation also implies a slight stiffness reduction of the soil in the upper part of the backfill side of the wall, the effect of the change of stiffness of the different layers in the ranges obtained from the DH tests in S6 was also investigated, leading to a finer refinement of the numerical model.

4.2 MODEL REFINEMENT FROM ANALYSIS OF THE INTERACTION AMONG THE GEOLOGICAL FORMATIONS

The analysis of the model geometry reveals that the retaining wall actually represents a boundary between the two halves of the system. It separates the geological formation in two

domains having a significant grade difference of about 8 m. The two domains of the system, if separately analyzed, show different dynamic properties.

The retaining wall, located at the boundary, depicts influences from both the domains, roughly represented by a superposition of the frequency responses of the two previously mentioned parts. In order to study the influence of the two domains, the spectral responses of the free-field motions in each of the areas are studied and compared to the overall response of the system. Considering the basic model, trials with different thickness of the bottom-most layer are carried out in order to get a better insight into the issue.

Table 4 enumerates the responses of the study. It can be observed that a rough superposition does hold, the dynamic response of the overall system being definitely guided by the natural frequencies of the soil domains on either sides of the wall. This observation provides useful suggestions about how to carry out the model refinement. Hence, the overall response of the system, which is a coupled problem, can be decoupled by controlling the dynamic response of the two soil domains, separately treated.

Thickness of bottom-most layer (m)	First two natural frequencies of vibration (Hz)		
	Dynamic response of the overall system measured on the wall	Free-field response of soil behind the wall	Free-field response of the soil in front of the wall
4	5.0, 8.0	5.1, 12.9	8.0, 16.7
10	4.6, 6.6	4.7, 10.8	6.6, 13.6
20	4.1, 5.2	4.0, 8.2	5.2, 11.0

Table 4. Dynamic response of the overall system and free-field responses of soil domains for different thickness of the bottom-most layer

Table 3 reveals significant scatter between the experimentally obtained frequencies and the numerical values from the basic model. According to the above-mentioned concept of decoupled responses, adjustments in the bed thickness were carried out to improve the model correlation with the experimental data. **Figure 6c** shows the geometry of the model after a first refinement. It is

characterized by thicker bed at the left of the wall and a comparatively thinner bed on its right, in agreement with the presence of hard soil recognized during the in-situ investigations. The connection between the two beds governs the actual dynamic superposition effect on the wall, and it was chosen by trial and guided by the frequency scatter. **Figure 6d** portrays the meshing of the adopted model; **Table 5** enumerates the material properties of the best model after the first refinement.

Table 3 also delivers a comparison between the dynamic properties obtained from the experimental investigations and the numerical predictions after the first refinement. The refined model has, therefore, provided results characterized by reduced frequency scatter, and as such it could be referred to as fairly representative of the actual behavior of the system in operational conditions. However, scrutiny of mode shapes revealed a reversal of the modes obtained from the numerical model with respect to those provided by ambient vibration tests. In fact, the highest MAC values were located on the anti-diagonal of the 2-by-2 MAC matrix between the experimental and numerical mode shapes.

First refinement							
Soil Layer	Material Type	E_{0L} (10^5 kPa)	E_{0R} (10^5 kPa)	ν	γ (kN/m ³)	H_L (m)	H_R (m)
A	LE	1.704	3.188	0.432	18.00	8	3
B	LE	2.930	4.086	0.426	19.03	3	3
C	LE	14.86	14.51	0.438	19.47	5	5
D	LE	26.49	26.49	0.433	19.98	20	4
Second refinement							
Soil Layer	Material Type	E_{0L} (10^5 kPa)	E_{0R} (10^5 kPa)	ν	γ (kN/m ³)	H_L (m)	H_R (m)
A	LE	1.565	3.188	0.432	18.00	8	3
B	LE	3.482	4.086	0.426	19.03	3	3
C	LE	14.86	14.51	0.438	19.47	5	5
D	LE	26.49	26.49	0.433	19.98	19	35

Table 5. Material properties adopted in the FE model after the first and second refinement (L= left side of the wall), (R= right side of the wall)

The observed inversion depended on the chosen geometry of the model. The initial choice was guided by the presence of hard soil on the excavated side at a depth of about 15 m. Another refinement to the model was carried out wherein the thickness of the base layer on the left side is less in comparison to the right side, and hence, the connection in the base layer is downward sloping from left to right. **Figure 6e** reports the geometry of the model, while the adopted meshing is portrayed in **Figure 6f**. **Table 5** provides the material properties adopted in the model after the second refinement.

Table 6 shows the comparison of the dynamic properties obtained from the model after the second refinement and the corresponding experimental estimates. The scatter in terms of frequencies was substantially reduced with respect to the basic model (**Table 3**) and the correlation was improved also in comparison to the first refined model (**Table 3**). In particular, the results reported in **Table 3** and **Table 6** represent the best correlation as provided by sensitivity analyses with respect to the updating parameters, including the elastic properties of the two upper layers in the backfill side of the wall. A little stiffness decrease with respect to the corresponding layers on the excavated side was required to optimize the correlation. After the second refinement, the mode inversion was no more observed and a high correlation between numerical and experimental mode shapes, pointed out by MAC values very close to 1 (**Table 6**), was obtained.

Mode	f_{exp} (Hz)	f_{FEM} (Hz)	Scatter (%)	MAC
I	3.68	3.65	-0.81	0.994
II	7.23	7.32	1.24	0.997

Table 6. Correlation between experimental and numerical estimates of the dynamic properties: FE model after the second refinement

5 CONCLUSIONS

The dynamic response of embedded retaining walls is not frequently investigated in geotechnical engineering. However, the recent seismic events in urban areas dredged out the necessity to enhance the knowledge about the dynamic behavior of such structures.

The present paper discussed about the use of the measurements of the natural frequencies and the modal shapes of an embedded retaining wall to get a representative model of in operational conditions after a process of refinement. According to the results of geotechnical investigations, a basic numerical model was set and its dynamic response was analyzed. The main sources of uncertainty were identified and the numerical model was refined by optimizing the correlation between experimental and numerical estimates of the dynamic properties of the soil-wall system. The resulting model can be, therefore, referred to as representative of the real system in its operational conditions. The mutual influence of retained and excavated side of the wall was documented and a superposition principle accordingly validated, resulting in a potential a priori estimation of the response of the overall system based on the knowledge of the decoupled responses of different domains defined by the excavation.

The results of the study are certainly promising and encouraging in view of their extension to the simulation of the response of the system under seismic excitation through the adoption of more advanced soil constitutive models and taking advantage of measurements of the wall response to eventual ground motions occurring in the area.

ACKNOWLEDGMENTS

The present research was partially supported by the ReLuis-DPC Executive Project 2014-2016, Special Project “Monitoring”, whose contribution is gratefully acknowledged. Support of the 2008 Italian Ministry of Education “Indian-fellowship” program and the University of Molise to Dr. Dey’s post-doc research fellowship is also gratefully acknowledged.

REFERENCES

- [1] Coulomb, C.A. (1776). “Essai sur une application des regles des maximis et minimis a quelques problemes de statique relatifs a l'architecture”. Memoires de l'Academie Royale pres Divers Savants, 7.

-
- [2] Rankine, W. (1857). "On the stability of loose earth". Philosophical Transactions of the Royal Society of London, 147.
- [3] Okabe, S. (1926). "General theory of earth pressures", Journal of the Japan Society of Civil Engineering, 12(1).
- [4] Mononobe, N. and Matsuo, H. (1929). "On the determination of earth pressure during earthquakes". Proceedings of the World Engineering Conference, Vol. 9, Tokyo, Japan, 177-185.
- [5] Veletsos, A.S. and Younan, A.H. (1997). "Dynamic response of cantilever retaining walls". ASCE Journal of Geotechnical and Geoenvironmental Engineering, 123(2), 161–172.
- [6] Koseki, J., Tatsuoka, F., Munaf, Y., Tateyama, M. and Kojima, K. (1997). "A modified procedure to evaluate active earth pressure at high seismic loads". Soils and Foundations, Special Issue on Geotechnical Aspects of the January 17 1995 Hyogoken-Nambu Earthquake, 209-216.
- [7] Nakamura, S. (2006). "Reexamination of Mononobe-Okabe theory of gravity retaining walls using centrifuge model tests". Soils and Foundations, 46(3), 135-146.
- [8] Mylonakis, G., Kloukinas, P. and Papantonopoulos, C. (2007). "An alternative to the Mononobe–Okabe equations for seismic earth pressures". Soil Dynamics and Earthquake Engineering, 27(10), 957–969.
- [9] NCHRP - National Cooperative Highway Research Program (2008). "Seismic Analysis and Design of Retaining Walls, Buried Structures, Slopes, and Embankments". Transportation Research Board, Report 611, pp. 137.
- [10] Seed, H.B. and Whitman, R.V. (1970). "Design of earth retaining structures for dynamic loads". Proceedings of Specialty Conference on Lateral Stresses in the Ground and Design of Earth Retaining Structures, American Society of Civil Engineers, Ithaca, New York, USA, 103-147.
- [11] EN 1998-5 - Eurocode 8 Part 5 (2003). "Design of structures for earthquake resistance – Part 5: Foundations, retaining structures and geotechnical aspects". CEN European Committee for Standardization, Bruxelles, Belgium.
- [12] NTC (2008). "Nuove Norme Tecniche per le Costruzioni", D.M. Infrastrutture 14/01/2008, Consiglio Superiore dei Lavori Pubblici, published on S.O. n. 30 at the G.U. 04/02/2008 n. 29 (in Italian).
- [13] FEMA - Federal Emergency Management Agency (2009). "NEHRP Recommended Seismic Provisions for Seismic Regulation of Buildings and Other Structures", FEMA P-750,

-
- prepared for FEMA by the Building Seismic Safety Council. Federal Emergency Management Agency, Washington, D.C.
- [14] Ebeling, R.M. and Morrison, E.E. (1992). "The Seismic Design of Waterfront Retaining Structures". Technical Report ITL-92-11. Vicksburg, Mississippi: Corps of Engineers Waterways Experiment Station.
- [15] Giarlelis, C. and Mylonakis, G. (2011). "Interpretation of dynamic retaining wall model tests in light of elastic and plastic solutions". *Soil Dynamics and Earthquake Engineering*, 31(1), 16-24.
- [16] Amano, R., Azuma, H. and Ishii, Y. (1956). "Aseismic Design of Quay Walls in Japan". *Proceedings of The First World Conference on Earthquake Engineering*, Berkeley, California, pp. 32-1, 32-17.
- [17] Fukuoka, M. and Imamura, Y. (1985). "Researches on retaining walls during earthquake". *Proceedings of The 8th World Conference on Earthquake Engineering*, Vol. 3, San Francisco, CA, USA, 501-508.
- [18] Elgamal, A.-W., Alampalli, S. and Van Laak, P. (1996). "Forced Vibration of Full-Scale Wall Backfill System". *ASCE Journal of Geotechnical and Geoenvironmental Engineering*, 122(10), 849-858.
- [19] Richart, F.E., Hall, J.R. and Woods, R.D. (1970). "Vibrations of soils and foundations", Prentice-Hall, Englewood Cliff, New Jersey.
- [20] Fabbrocino, G., Laorenza, C., Rainieri, C. and Santucci de Magistris, F. (2009). "Seismic monitoring of structural and geotechnical integrated systems". *Materials Forum*, 33, 404-419.
- [21] Rainieri, C., Fabbrocino, G. and Santucci de Magistris, F. (2013). "An integrated seismic monitoring system for a full- scale embedded retaining wall". *Geotechnical Testing Journal*, 36(1), 1–15.
- [22] Brincker, R., Zhang, L. and Andersen, P. (2001). "Modal identification of output-only systems using frequency domain decomposition". *Smart Materials and Structures*, 10, 441-445.
- [23] Rainieri, C. and Fabbrocino, G. (2014). "Operational Modal Analysis of Civil Engineering Structures: An Introduction and Guide for Applications", Springer, New York.
- [24] Van Overschee, P. and De Moor, B. (1996). "Subspace identification for linear systems: Theory – Implementation – Applications", Kluwer Academic Publishers, Dordrecht, The Netherlands.

-
- [25] Peeters B. (2000). "System identification and damage detection in civil engineering", Ph.D. Thesis, Katholieke Universiteit Leuven, Leuven, Belgium.
- [26] Brinkgreve, R.B. (2002). "Plaxis 2D Version 8.4: Reference, Scientific and Dynamics Manuals", Balkema, Lisse, The Netherlands.
- [27] Visone, C., Bilotta, E. and Santucci de Magistris, F. (2010). "One-dimensional ground response as a preliminary tool for dynamic analyses in Earthquake Geotechnical Engineering". *Journal of Earthquake Engineering*. 14(1), 131 – 162.
- [28] Lysmer, J. and Kuhlemeyer, R.L. (1969). "Finite dynamic model for infinite media". *Journal of Engineering Mechanics Division Proceedings ASCE* 95(EM4), 859-877.
- [29] Kuhlemeyer, R.L. and Lysmer, J. (1973). "Finite element method accuracy for wave propagation problems". *Journal of the Soil Mechanics and Foundations Division Proceedings ASCE* 99(SM5), 421-427.
- [30] Bendat, J.S. and Piersol, A.G. (2000). "Random data: analysis and measurement procedures", 3rd edn., John Wiley & Sons, New York, USA.
- [31] Barrios, D.B., Angelo, E. and Goncalves, E. (2005). "Finite element shot peening simulation for residual stress analysis and comparison with experimental results". *Mecànica Computacional*, 3(XXIV), 413-422.
- [32] LUSAS (2000). "Theory Manual", FEA Ltd, United Kingdom.
- [33] Park, D. and Hashash, Y.M. (2004). "Soil damping formulation in nonlinear time domain site response analysis". *Journal of Earthquake Engineering*, 8(2), 249-274.
- [34] Ewins, D.J. (2000). "Modal Testing: Theory, Practice and Application", 2nd edn. Research Studies Press Ltd., Baldock.
- [35] Friswell, M.I. and Mottershead, J.E. (1995). "Finite Element Model Updating in Structural Dynamics", Kluwer Academic Publishers, Dordrecht, The Netherlands.
- [36] Mottershead, J.E., Link, M. and Friswell, M.I. (2010). "The sensitivity method in finite element model updating: A tutorial". *Mechanical Systems and Signal Processing*, 25(7), 2275-2296.
- [37] Allemang, R.J. and Brown, D.L. (1982). "A correlation coefficient for modal vector analysis". *Proceedings of the 1st SEM International Modal Analysis Conference*, Orlando, FL, USA.

1 List of Figures

- Figure 1 Picture view of part of the geotechnical works for the New Students' Residence in Campobasso (a); layout of the equivalent sheet pile cross section, plan view (b)
- Figure 2 Geological map and section of the Vazzieri area in Campobasso. *AVS* – Varicolored scaly clays; *ter2* – Deposits of debris cover; *anf2* – Anthropogenic remolded covering; *SAN2* – San Bartolomeo's Flysch deposit (a); schematic location of boreholes and retaining wall on a contour plot; the general direction of slope in the locality is indicated by the arrow (b); characteristics of strata and SPT test results for Borehole S6 (c) and Borehole S5 (d)
- Figure 3 Shear wave velocity profile obtained from borehole S5 (a) and borehole S6 (b)
- Figure 4 Sensor layout
- Figure 5 Analysis of the ambient vibration response of the wall: Singular value plots from the FDD method (a), stabilization diagram from the SSI method (b), first experimental mode shape (c), second experimental mode shape (d)
- Figure 6 Views of the FE models in the region around the wall: Geometry of the basic FE model (a) and its zoomed meshing (b); zoomed view of the FE model geometry after the first refinement (c) and its meshing (d); zoomed view of the FE model geometry after the second refinement (e) and its meshing (f)
- Figure 7 Conglomerated plot of SPT blow-counts from the nearby boreholes towards the soil in front of the wall as a function of depth from the ground level

1 List of Tables

2

Table 1	Experimental estimates of natural frequencies and damping ratios in operational conditions
Table 2	Material properties of soil adopted in the basic FE model
Table 3	Comparisons between experimental and numerical estimates of the natural frequencies: the basic FE model and the FE model after the first refinement
Table 4	Dynamic response of the overall system and free-field responses of soil domains for different thickness of the bottom-most layer
Table 5	Material properties adopted in the FE model after the first and second refinement (L= left side of the wall), (R= right side of the wall)
Table 6	Correlation between experimental and numerical estimates of the dynamic properties: FE model after the second refinement